ACS Photonics

Article

pubs.acs.org/journal/apchd5

Trapping and Guiding Surface Plasmons in Curved Graphene Landscapes

Daria Smirnova,[†] S. Hossein Mousavi,[‡] Zheng Wang,[‡] Yuri S. Kivshar,[†] and Alexander B. Khanikaev*[,§,⊥]

[†]Nonlinear Physics Center, Australian National University, Canberra, ACT 2601, Australia

[‡]Microelectronics Research Center, Cockrell School of Engineering, University of Texas at Austin, Austin, Texas 78758, United States

[§]Department of Physics, Queens College of The City University of New York, Queens, New York 11367, United States

[⊥]Department of Physics, The Graduate Center of The City University of New York, New York, New York 10016, United States

ABSTRACT: We demonstrate that graphene placed on top of curved substrates offers a novel approach for trapping and guiding surface plasmons. Monolayer graphene with a spatially varying curvature exhibits an effective trapping potential for graphene plasmons near curved areas such as bumps, humps, and wells. We derive the governing equation for describing such localized channel plasmons guided by curved graphene and validate our theory by first-principle numerical simulations. The proposed confinement mechanism enables plasmon guiding by the regions of maximal curvature, and it offers a versatile platform for manipulating light in planar landscapes. In addition, isolated deformations of graphene such as bumps are shown to support localized surface modes and resonances, suggesting a new way to engineer graphene-based metasurfaces.

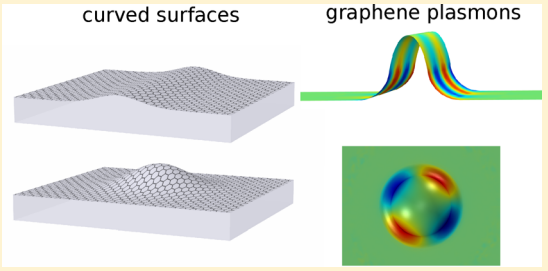

KEYWORDS: *graphene plasmons, curvature, trapping potential*

Unprecedented optical properties make graphene a promising plasmonic material with great potential for practical applications ranging from optical routing[1−5] to nonlinear optics,[6] optomechanics,[7] and sensing.[8] In addition to the relatively strong and tunable electromagnetic response of this one-atom-thick material, it was shown that at infrared frequencies graphene supports surface plasmon-polaritons (SPPs) with extreme confinement and propagation characteristics controllable by doping.[9] In particular, thanks to the strong dependence of its optical characteristics from electric bias, graphene is on the path to be widely used for electro-optical modulation.[1,10] The possibility of electrostatic doping enables an efficient control over the electron density at the Fermi level, which defines the high-frequency optical response of graphene.[11−15] With tremendous success in graphene electronics, these unique capabilities enable integration of plasmonic and electronic devices on the same substrate[16−20] and even the design of tunable cloaking devices.[21]

Presently, two of the most common approaches to utilize the unique plasmonic response of graphene for guiding applications rely on (i) inhomogeneous gating of graphene[22,23] affecting its local plasmonic response and (ii) subwavelength-scale patterning of the graphene layer, giving rise to localized plasmonic resonances.[5]

In this paper, we propose *an alternative approach* to engineer plasmonic guiding properties of graphene by employing its property to confine and scatter light by curved regions such as extended one-dimensional humps and local two-dimensional deformations. Technologically, such curved graphene profiles, shown schematically in Figure 1a,b, can be either fabricated by transferring graphene onto curved dielectric substrates or grown directly by laser ablation on the structured surface of SiC demonstrated recently.[24] In particular, we demonstrate plasmon guiding by a bump of monolayer graphene, which effectively operates as a plasmonic channel waveguide.[25−33] In addition, we show that a local isolated deformation of graphene in the form of a bump supports local surface plasmonic

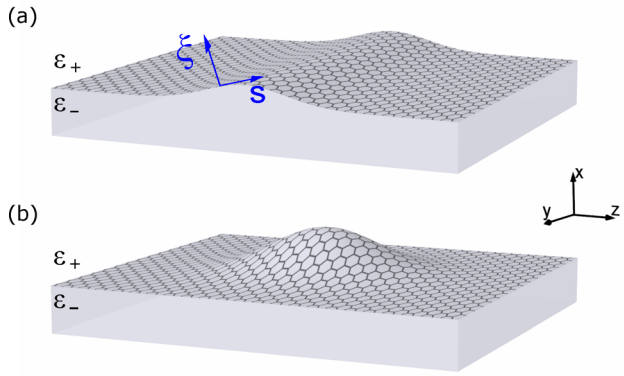

Figure 1. Schematic view of convex curved substrates covered by graphene and related global Cartesian and local curvilinear coordinate systems. (a) and (b) correspond to the cases of one- and two-dimensional curved surfaces, respectively.

Received: February 17, 2016
Published: March 22, 2016

DOI: 10.1021/acsphotonics.6b00116
ACS Photonics 2016, 3, 875−880

resonances. The localized plasmonic modes studied here differ from the modes supported by gratings that can be generated in graphene by acoustic or elastic waves.[34,35]

It has been already established that a curved graphene surface can play a role of an effective potential for electrons and phonons; for example, it may support spatially localized phonons.[36] Similarly, we may expect that graphene plasmons can be modified by effective geometric potentials, as this was shown earlier for curved metal−dielectric interfaces.[37] We notice that the study of the propagation of light in curved dielectric space has attracted some special attention due to novel opportunities to guide and focus light.[38−40] Here, we extend these ideas to the case of plasmons in curved graphene and demonstrate substantially different regimes for engineering plasmons in curved graphene.

RESULTS AND DISCUSSION

Analytical Approach. As the first step, we explore the capability of trapping light with the use of an analytical approach assuming a graphene surface of small one-dimensional curvature. Specifically, we consider a graphene monolayer placed on a curved interface between two dielectric media with permittivities ε_- and ε_+, as shown in Figure 1a. Such a graphene-coated surface forms a channel waveguide for surface plasmons, thus enabling a two-dimensional (2D) spatial localization of light, alternative to waveguides created by graphene conductivity modulation.[22,23] We base our analytical consideration on Maxwell's equations solved in the adiabatic approximation within the small-wavelength limit.

We assume that an inhomogeneity in the graphene profile is described by a smooth function $x = f(z)$, and we look for modes propagating along the y axis. For convenience, the curvilinear orthogonal coordinate system $\{\xi, y, s\}$ bound to the reference curve $x = f(z)$ is used in place of the Cartesian coordinate system $\{x, y, z\}$. Accepting harmonic $\exp(-i\omega t)$ time-dependence, Maxwell's equations can be written as follows:

$$\begin{cases} \nabla \times \mathbf{E} = ik_0\mathbf{H}, \\ \nabla \times \mathbf{H} = -ik_0\varepsilon(\xi)\mathbf{E} + \dfrac{4\pi}{c}\delta(\xi)\,\sigma(\omega)\mathbf{E}_\tau \end{cases} \tag{1}$$

where $k_0 = \omega/c$ is the wavenumber in free space, $\sigma(\omega) \equiv i\sigma^{(I)}(\omega) + \sigma^{(R)}(\omega)$ is the linear frequency-dependent surface conductivity of graphene, and the function $\varepsilon(\xi)$ describes the dielectric permittivity distribution,

$$\varepsilon(\xi) = \begin{cases} \varepsilon_-, & \xi < 0 \\ \varepsilon_+, & \xi > 0 \end{cases} \tag{2}$$

The Dirac delta function $\delta(\xi)$ in eq 1 indicates that the graphene layer is placed at $\xi = 0$, and the subscript τ refers to the field component tangential to the surface. In our case of low-energy excitations close to the Dirac points, where transitions occur within the $\pi-\pi^*$ electronic bands, the normal component of the induced current density in graphene is negligible. The marginal character of the contribution normal to the surface is also evidenced by the earlier experimental studies.[41]

Equation 1 leads to

$$\begin{aligned} &-\nabla \times \nabla \times \mathbf{H} + k_0{}^2\varepsilon(\xi)\mathbf{H} \\ &\quad = ik_0\nabla\varepsilon(\xi) \times \mathbf{E}_\tau - \frac{4\pi}{c}\sigma(\omega)\nabla \times \delta(\xi)\mathbf{E}_\tau \end{aligned} \tag{3}$$

where $\mathbf{E}_\tau = \frac{i}{k_0\varepsilon(\xi)}(\nabla \times \mathbf{H})_\tau$ is continuous at $\xi = 0$, and the vector operations can be calculated using the Lame coefficients given as $h_\xi = 1$, $h_y = 1$, $h_s = 1 - \varkappa(s)$, $\xi \equiv 1 - \xi/R$, where $\varkappa(s) \approx f''(z)$ is a signed curvature of the reference cylinder line $x = f(z)$ and $R = 1/\varkappa(s)$ is the local radius of curvature.

Following the approach elaborated earlier in refs 42−45 we derive the equation for the slowly varying plasmon amplitude, employing the asymptotic description often used in the paraxial optics and physics of optical solitons.[46] To develop the consistent perturbation theory, we introduce a small parameter,

$$\beta^2 = \max\left\{\frac{1}{k_{sp}|R|}, \left|\frac{\sigma^{(R)}}{\sigma^{(I)}}\right|\right\}$$

assuming the losses in graphene and spatial inhomogeneity to be small ($\beta^2 \ll 1$). Accordingly, the solution of eq 3 is sought in the form

$$\begin{aligned} H_s &= [A(\beta^2 y, \beta s)h(\xi) + \beta^2 \mathrm{H}^{(2)}(\beta^2 y, \beta s, \xi) + ...]\mathrm{e}^{ik_{sp}y} \\ &= [\mathcal{A}(s, y)h(\xi) + H^{(2)}(s, y, \xi) + ...]\mathrm{e}^{ik_{sp}y}, \\ H_y &= [\beta H^{(1)}(\beta^2 y, \beta s, \xi) + \beta^3 \mathrm{H}^{(3)}(\beta^2 y, \beta s, \xi) + ...]\mathrm{e}^{ik_{sp}y} \\ &= [H^{(1)}(s, y, \xi) + H^{(3)}(s, y, \xi) + ...]\mathrm{e}^{ik_{sp}y} \end{aligned} \tag{4}$$

where $\mathcal{A}(s, y)$ is the slowly varying amplitude of the plasmonic mode propagating along the curved channel and $k_{sp}(\omega)$ satisfies the dispersion relation

$$\frac{\varepsilon_+}{\kappa_+} + \frac{\varepsilon_-}{\kappa_-} = \frac{4\pi}{\omega}\sigma^{(I)}(\omega) \tag{5}$$

where $\kappa_{+,-} = (k_{sp}^2 - k_0^2\varepsilon_{+,-})^{1/2}$.

Substituting eqs 4 into eq 3 and maintaining zeroth-order terms in β leads to the dispersion relation 5 and gives the transverse profile for the plasmon on a locally flat graphene,

$$h(\xi) = -ik_0\begin{cases} \dfrac{\varepsilon_+}{\kappa_+}\mathrm{e}^{-\kappa_+\xi} & (\xi > 0) \\ -\dfrac{\varepsilon_-}{\kappa_-}\mathrm{e}^{\kappa_-\xi} & (\xi < 0) \end{cases} \tag{6}$$

The correction $H^{(1)}$ of the first order in β is determined from $\nabla\cdot\mathbf{H} = 0$ as $H^{(1)} = (i/k_{sp})(\partial\mathcal{A}/\partial s)h(\xi)$.

The second-order correction $H^{(2)}$ for $\xi \neq 0$ satisfies

$$\begin{aligned} &\frac{\mathrm{d}^2H^{(2)}}{\mathrm{d}\xi^2} + (k_0^2\varepsilon(\xi) - k_{sp}^2)H^{(2)} = F \\ &F = -\left(2ik_{sp}\frac{\partial\mathcal{A}}{\partial y} + \frac{\partial^2\mathcal{A}}{\partial s^2}\right)h(\xi) - \varkappa(s)\mathcal{A}\frac{\partial h}{\partial\xi} \end{aligned} \tag{7}$$

By imposing the boundary conditions on solutions of eq 7 at the interface $\xi = 0$,

$$\begin{aligned} &E_y^{(2)}(\xi = +0) = E_y^{(2)}(\xi = -0) \equiv E_y^{(2)} \\ &H^{(2)}(\xi = +0) - H^{(2)}(\xi = -0) \\ &\quad = -\frac{4\pi}{c}(\sigma^{(R)}(\omega)\mathcal{A} + i\sigma^{(I)}(\omega)E_y^{(2)}) \end{aligned}$$

where

DOI: 10.1021/acsphotonics.6b00116
ACS Photonics 2016, 3, 875−880

$$E_y^{(2)}(\xi = \pm 0) = \frac{1}{ik_0\varepsilon_\pm}\frac{\partial H^{(2)}}{\partial \xi}(\xi = \pm 0) - \frac{1}{R\kappa_\pm}\mathcal{A}$$

we find that the amplitude $\mathcal{A}$ of the plasmon satisfies the equation

$$2ik_{sp}\left(\frac{\partial \mathcal{A}}{\partial y} + \gamma\mathcal{A}\right) + \frac{\partial^2\mathcal{A}}{\partial s^2} - g(s)\mathcal{A} = 0 \quad (8)$$

where the damping coefficient γ is expressed as

$$\gamma = \frac{\frac{4\pi}{\omega}\sigma^{(R)}(\omega)}{\left(\frac{\varepsilon_-}{\kappa_-^3} + \frac{\varepsilon_+}{\kappa_+^3}\right)k_{sp}}$$

and the curvature-dependent function $g(s)$,

$$g(s) = \varkappa(s)\left(\frac{\varepsilon_+}{\kappa_+^2} - \frac{\varepsilon_-}{\kappa_-^2}\right)\left(\frac{\varepsilon_+}{\kappa_+^3} + \frac{\varepsilon_-}{\kappa_-^3}\right)^{-1}$$

is an effective geometric potential for plasmons.[37]

Remarkably, the result of ref 37 for plasmons at a curved metal−dielectric interface can be retrieved from eq 8 by setting $\sigma(\omega) = 0$ and assuming that the substrate possesses a plasma-like frequency-dependent dielectric permittivity ε_-. In this case $\varepsilon_-/\kappa_- = -\varepsilon_+/\kappa_+$, that leads to $g(s) = -R^{-1}\frac{\kappa_+\kappa_-}{\kappa_+ - \kappa_-} = R^{-1}\frac{k_{sp}^2}{k_0}\left(-\frac{1}{\varepsilon_+ + \varepsilon_-}\right)^{1/2}$. Besides, the case of a constant curvature describes TM plasmons propagating along cylindrical graphene-coated nanowires.[47]

As follows from eq 8, the symmetric dielectric environment, $\varepsilon_- = \varepsilon_+ = \varepsilon$, suggests $g(s) = 0$ and implies that no localization to the curved region is possible in the case of 1D curvature, while the loss coefficient is found to be $\gamma = \frac{2\pi}{k_{sp}\omega}\sigma^{(R)}(\omega)\frac{\kappa^3}{\varepsilon}$, which is in agreement with that calculated earlier in refs 44 and 45, where the equation for the correction $H^{(2)}$ is written with incorporated boundary conditions using the formalism of δ functions.

As an example, we consider the interface profile of the Gaussian form. This results in inhomogeneous curvature, which at some parts becomes a potential well capable of confining a mode. In our calculations, graphene is described by the surface conductivity written in terms of the Drude model $\sigma(\omega) = (ie^2/\pi\hbar^2)\mathcal{E}_F(\omega + i\tau_{intra}^{-1})^{-1}$, where the Fermi energy $\mathcal{E}_F = 0.307$ eV and $\tau_{intra} = 0.5$ ps is the relaxation time. This case of doped graphene satisfying $\hbar\omega < \mathcal{E}_F$ allows neglecting the interband transitions and temperature effects.[12] The propagation distance for plasmons in this case can be as large as 16 plasmon wavelengths (~13.5 μm). However, the approximation employing a local conductivity function has its range of applicability, since the curvature may affect electronic properties of graphene.[48] By using the approach of ref 48 to estimate the pseudomagnetic field induced by graphene strain, we assume that this field is proportional to the curvature and estimate the cyclotron energy to be $\hbar\omega_c \leq 0.02$ eV for typical smooth surface profiles with the scales of a few hundred nanometers considered here. This number is significantly lower than the frequencies of plasmonic surface waves (0.06−0.15 eV) studied here. Therefore, we do not expect the strain to affect the dispersion of plasmons in our systems.

The confining potential corresponding to the Gaussian channel operates as a 2D plasmonic waveguide with trapped modes being eigenstates of the stationary Schrödinger-like eq 8, shown in Figure 2. The first example considered here corresponds to the substrate dielectric constant exceeding that of the superstrate. Only one bound state is found for the given set of parameters with its amplitude spatial dependence $\mathcal{A}(z, y) = a(z)\exp(i\Delta k_{sp}y)$. The position of eigenvalue Δk_{sp}

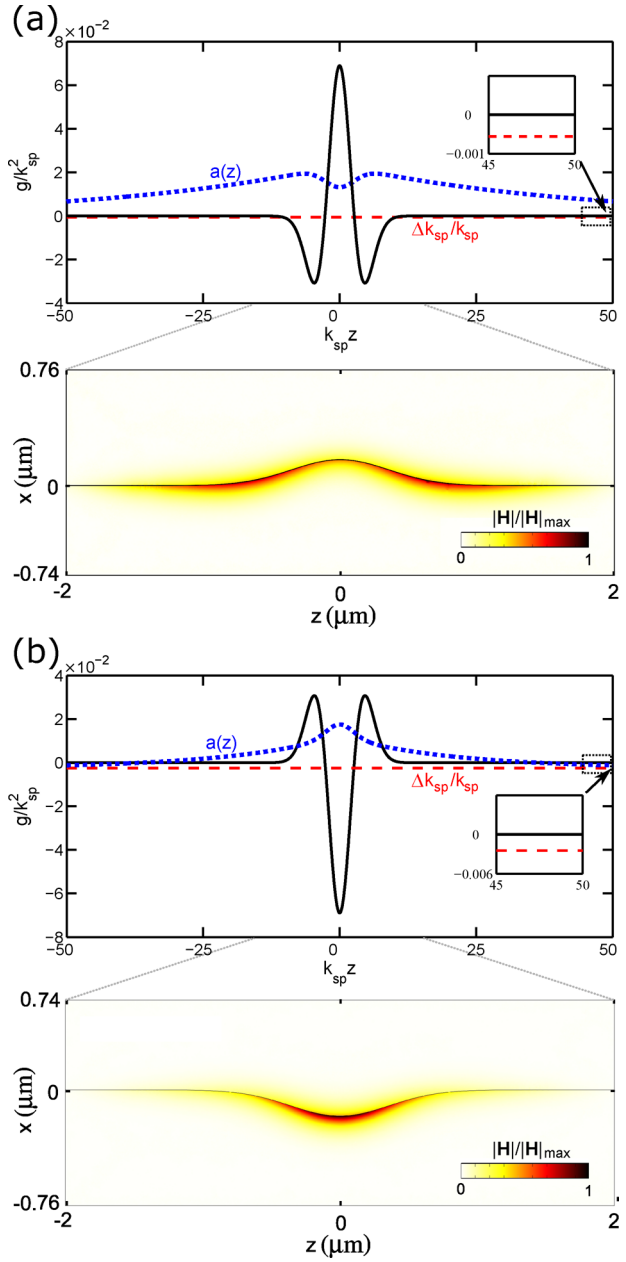

Figure 2. Top panels in (a) and (b): Effective potential (black solid curves) and transverse profiles $a(z)$ (au) of the trapped modes (blue dotted curves) calculated for the Gaussian profiles $f(z) = \pm f_0\exp(-z^2/w^2)$, $f_0 = 200$ nm, $w = 506$ nm, and dielectric permittivities $\varepsilon_+ = 1$, $\varepsilon_- = 2$ at the frequency $\omega_0/2\pi = 16$ THz, respectively. The red dashed line levels the relative correction $\Delta k_{sp}/k_{sp}(\omega_0)$ to the wavenumber $k_{sp}(\omega_0) = 22.4$, k_0 corresponding to the fundamental channel mode. Bottom panels in (a) and (b): Normalized magnetic field distribution $|\mathbf{H}|/|\mathbf{H}|_{max}$ of the modes shown in the top panels and obtained with the use of a first-principle FEM solver.

DOI: 10.1021/acsphotonics.6b00116
ACS Photonics 2016, 3, 875−880

with respect to the trapping potential is indicated in Figure 2a (top panel, red dashed line). The state appears to be less localized to the curved region, with the fields primarily located near the side regions of maximal positive curvature. The second case studied has an inverted profile and also supports one localized state illustrated in Figure 2b, top panel. One can see that for this case the field is mainly localized at the central dip (notch) having the maximal positive curvature and exhibits quite strong localization in the in-plane transverse z direction. Despite the approximation made in the derivation of the analytical theory, we found that its applicability extends beyond these limits. In particular, the case shown in Figure 2 compares the results of analytical and first-principles calculations, which appear to agree extremely well even for the value of small parameter $\beta^2 \approx 0.2$.

We emphasize that in the present work we focus exclusively on the effect of the geometrical potential, thus assuming that graphene is chemically doped and has uniform distribution of the Fermi energy $\mathcal{E}_F$ over its surface. The effect of a small change in $\mathcal{E}_F$ on trapped modes is the same as that for conventional plasmons on a flat graphene layer. In both cases reduction in the surface conductivity leads to a stronger confinement of the plasmons. However, at any given frequency, as long as the change in the propagation constant caused by the deviation in the Fermi energy is small in comparison with the unperturbed wavenumber, it does not disrupt the described trapping mechanism for plasmons in curved graphene. Note that the sensitivity of the plasmons trapped by such geometric potential to changes in the Fermi energy is mainly stemming from the zeroth order contribution to the wavenumber k_{sp} in small parameter β. While the trapping mechanisms caused by nonuniform distribution of doping have been reported earlier,[22,23] here we demonstrate that nonuniform gating is not at all necessary to confine plasmons in lateral dimensions, and the curvature alone can be sufficient for many practical applications. Nevertheless, it might be of interest to endow such systems with additional functionalities, for example, tunability, by combining the geometric potential with that induced by the electrostatic gating. It is straightforward to expand our model to account for small variations of the graphene conductivity caused by graphene gating of curved substrates, by introducing an additional correction associated with a coordinate-dependent conductivity. This correction may modify the focusing properties dictated by the curvature and bring desirable controllability of plasmons.

Numerical Approach. To validate the developed analytical theory, first-principles numerical simulations are performed with the use of commercial full-vector FEM solver COMSOL Multiphysics. The graphene is modeled by the surface current tangential to the curved interface between the substrate and the superstrate: $\mathbf{j} = \sigma \mathbf{E}_\tau$. The numerical results, shown in Figure 2a,b, bottom panel, are found to be in excellent agreement with the results of our analytical theory.

While the applicability of our analytical model is restricted by its perturbative nature and small curvatures, the possibility to confine light with the curvature extends beyond this case. Moreover, the transverse in-plane confinement of the channel modes can be further improved when the curvature is increased. To localize the mode, any of the channel dimensions should be comparable to or exceed the wavelength of surface plasmons on a flat graphene layer. The particular cases of guiding by the strongly curved nonanalytic graphene profiles are given in Figure 3a,b. Similar to the case of small curvatures,

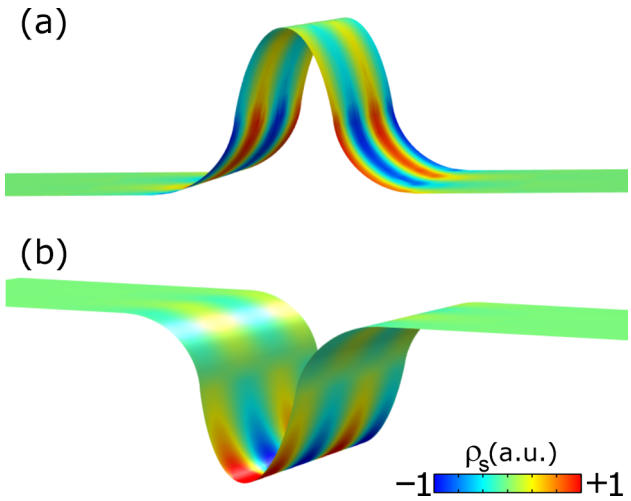

Figure 3. Channel waveguide modes found for the value of graphene conductivity $\sigma = 0.00035i$ S using the FEM method for $\varepsilon_+ = 1$, $\varepsilon_- = 2$: shown is the surface charge density distribution ρ_s on the curved graphene surface. The frequencies of the eigenmodes plotted in (a) and (b) are 21.1 THz and 23.9 THz, respectively. The geometrical parameters of the curved region are the height (depth) of the channel, which is 300 nm, and the width of the upper (lower) elliptical segment, which is 200 nm, and the radius of curvature of the two lower (upper) circular segments is 140 nm; the shown y-length is 1 μm.

the mode corresponding to graphene curved toward the high-index material shows more localized mode at the center of the curved region. As in any other open waveguiding system, any perturbation of the dielectric environment will lead to diffraction, scattering, and leakage of guided modes. However, as long as the perturbations are small and smooth enough on the scale of the plasmon wavelength, these effects will be negligible. Therefore, the guiding mechanism will be robust to the adiabatic changes in the width/height that happen on a scale larger than 1 μm.

The proposed concept of light trapping in curved graphene can be extended to the case of 2D profiles, such as circular channels and hemispherical bumps. The resultant structures possess cylindrical symmetry, and the trapped modes are quantized with respect to the azimuthal direction. Numerical results obtained in COMSOL by solving the full 3D FEM problem for both cases shown in Figure 4a,b reveal a variety of modes with increasing number of nodes as the frequency of the mode gradually increases. As opposed to the channel modes, and similar to the case of localized surface plasmons in metallic nanoparticles, these modes are leaky, and therefore they have a finite radiative lifetime.

CONCLUSION

We have suggested a novel approach to confine light in curved graphene landscapes. We have shown that curved graphene allows guiding surface plasmons trapped in the curved regions. With the modern techniques of graphene transfer and growth on prestructured substrates, our approach to confine and manipulate light with the curved surfaces can serve as a versatile platform for on-chip graphene plasmonics integration.

METHODS

Finite element method (FEM) calculations for a curved graphene waveguiding geometry were performed with the use of COMSOL Multiphysics eigensolver with periodic boundary

DOI: 10.1021/acsphotonics.6b00116
ACS Photonics 2016, 3, 875−880

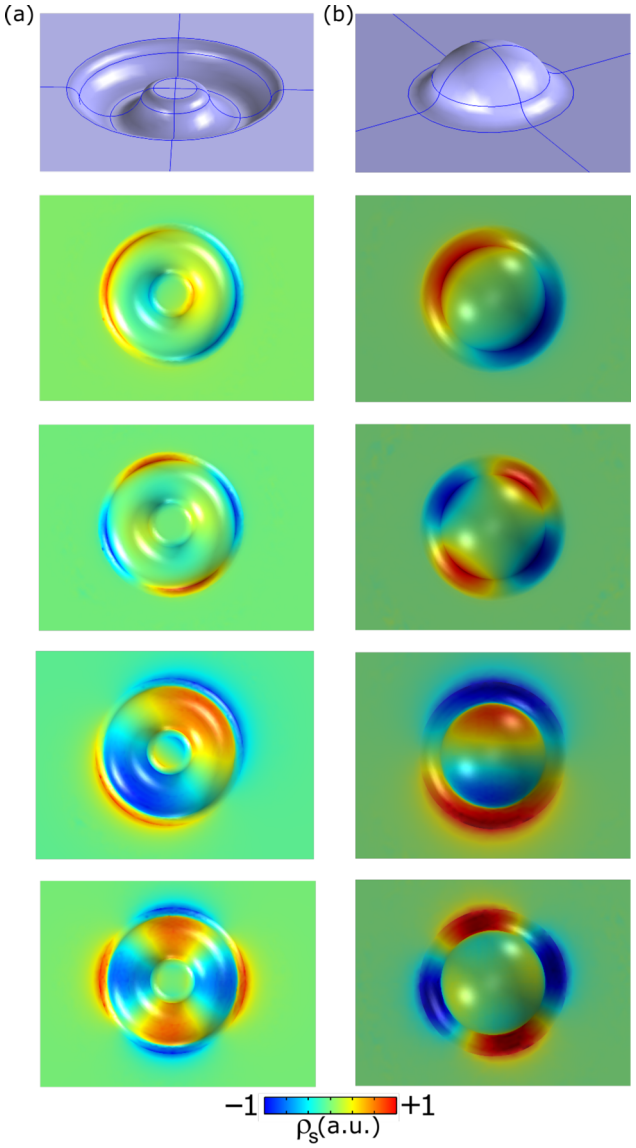

Figure 4. Geometry and localized modes of (a) circular channel (depth 100 nm, side curvature radius 33 nm) and (b) hemispherical bump (height 200 nm, side curvature radius 66 nm) found with the use of the FEM method. Upper panels in (a) and (b) show profiles of the curved regions. $\varepsilon_+ = 1$, $\varepsilon_- = 2$. The four lower panels in (a) and (b) depict the surface charge density distributions corresponding to the modes with increasing number of nodes in angular and radial directions. The eigenfrequencies found for the value of graphene conductivity $\sigma = 0.00035i$ S (from top to bottom): (a) 11.1, 14.4, 15.2, 21.8 THz; (b) 10.8, 14.5, 17.2, 22.8 THz.

conditions imposed in the y propagation direction and a cylindrical perfectly matched layer (PML) in the plane of curvature. Graphene was modeled as a surface current set on a curved interfacial surface. Localized graphene plasmons were simulated in a spherical shell of the PML.

AUTHOR INFORMATION

Corresponding Author

*E-mail: akhanikaev@qc.cuny.edu.

Notes

The authors declare no competing financial interest.

ACKNOWLEDGMENTS

This work was supported by the Australian Research Council and the Russian Foundation for Basic Research (grant 16-32-00635). The research used resources of the Center for Functional Nanomaterials, which is a U.S. DOE Office of Science Facility, at Brookhaven National Laboratory, under Contract No. DE-SC0012704. Z.W. acknowledges support from the Packard Fellowships for Science and Engineering and the Alfred P. Sloan Research Fellowship.

REFERENCES

(1) Grigorenko, A. N.; Polini, M.; Novoselov, K. S. Graphene plasmonics. *Nat. Photonics* **2012**, *6*, 749−758.
(2) Lozovik, Y. E. Plasmonics and magnetoplasmonics based on graphene and a topological insulator. *Phys.-Usp.* **2012**, *55*, 1035−1039.
(3) Jablan, M.; Soljacic, M.; Buljan, H. Plasmons in Graphene: Fundamental Properties and Potential Applications. *Proc. IEEE* **2013**, *101*, 1689−1704.
(4) Luo, X.; Qiu, T.; Lu, W.; Ni, Z. Plasmons in graphene: Recent progress and applications. *Mater. Sci. Eng., R* **2013**, *74*, 351−376.
(5) de Abajo, F. J. G. Graphene Plasmonics: Challenges and Opportunities. *ACS Photonics* **2014**, *1*, 135−152.
(6) Glazov, M.; Ganichev, S. High frequency electric field induced nonlinear effects in graphene. *Phys. Rep.* **2014**, *535*, 101−138.
(7) Mousavi, S. H.; Rakich, P. T.; Wang, Z. Strong THz and Infrared Optical Forces on a Suspended Single-Layer Graphene Sheet. *ACS Photonics* **2014**, *1*, 1107−1115.
(8) Rodrigo, D.; Limaj, O.; Janner, D.; Etezadi, D.; de Abajo, F. J. G.; Pruneri, V.; Altug, H. Mid-infrared plasmonic biosensing with graphene. *Science* **2015**, *349*, 165−168.
(9) Jablan, M.; Buljan, H.; Soljačić, M. Plasmonics in graphene at infrared frequencies. *Phys. Rev. B: Condens. Matter Mater. Phys.* **2009**, *80*, 245435.
(10) Liu, M.; Yin, X.; Ulin-Avila, E.; Geng, B.; Zentgraf, T.; Ju, L.; Wang, F.; Zhang, X. A graphene-based broadband optical modulator. *Nature* **2011**, *474*, 64−67.
(11) Wunsch, B.; Stauber, T.; Sols, F.; Guinea, F. Dynamical polarization of graphene at finite doping. *New J. Phys.* **2006**, *8*, 318−318.
(12) Falkovsky, L. A.; Varlamov, A. A. Space-time dispersion of graphene conductivity. *Eur. Phys. J. B* **2007**, *56*, 281−284.
(13) Chen, J.; Badioli, M.; Alonso-Gonzalez, P.; Thongrattanasiri, S.; Huth, F.; Osmond, J.; Spasenovic, M.; Centeno, A.; Pesquera, A.; Godignon, P.; Zurutuza Elorza, A.; Camara, N.; de Abajo, F. J. G.; Hillenbrand, R.; Koppens, F. H. L. Optical nano-imaging of gate-tunable graphene plasmons. *Nature* **2012**, *487*, 77−81.
(14) Fei, Z.; Rodin, A. S.; Andreev, G. O.; Bao, W.; McLeod, A. S.; Wagner, M.; Zhang, L. M.; Zhao, Z.; Thiemens, M.; Dominguez, G.; Fogler, M. M.; Neto, A. H. C.; Lau, C. N.; Keilmann, F.; Basov, D. N. Gate-tuning of graphene plasmons revealed by infrared nano-imaging. *Nature* **2012**, *487*, 82−85.
(15) Alonso-Gonzalez, P.; Nikitin, A. Y.; Golmar, F.; Centeno, A.; Pesquera, A.; Velez, S.; Chen, J.; Navickaite, G.; Koppens, F.; Zurutuza, A.; Casanova, F.; Hueso, L. E.; Hillenbrand, R. Controlling graphene plasmons with resonant metal antennas and spatial conductivity patterns. *Science* **2014**, *344*, 1369−1373.
(16) Bao, Q.; Loh, K. P. Graphene Photonics, Plasmonics, and Broadband Optoelectronic Devices. *ACS Nano* **2012**, *6*, 3677−3694.
(17) Mousavi, S. H.; Kholmanov, I.; Alici, K. B.; Purtseladze, D.; Arju, N.; Tatar, K.; Fozdar, D. Y.; Suk, J. W.; Hao, Y.; Khanikaev, A. B.; Ruoff, R. S.; Shvets, G. Inductive Tuning of Fano-Resonant Metasurfaces Using Plasmonic Response of Graphene in the Mid-Infrared. *Nano Lett.* **2013**, *13*, 1111−1117.
(18) Low, T.; Avouris, P. Graphene Plasmonics for Terahertz to Mid-Infrared Applications. *ACS Nano* **2014**, *8*, 1086−1101.

DOI: 10.1021/acsphotonics.6b00116
ACS Photonics 2016, 3, 875−880

(19) Chen, P.-Y.; Huang, H.; Akinwande, D.; Alù, A. Graphene-Based Plasmonic Platform for Reconfigurable Terahertz Nanodevices. *ACS Photonics* **2014**, *1*, 647−654.
(20) Forati, E.; Hanson, G. W.; Yakovlev, A. B.; Alù, A. Planar hyperlens based on a modulated graphene monolayer. *Phys. Rev. B: Condens. Matter Mater. Phys.* **2014**, *89*, 081410.
(21) Chen, P.-Y.; Soric, J.; Padooru, Y. R.; Bernety, H. M.; Yakovlev, A. B.; Alù, A. Nanostructured graphene metasurface for tunable Terahertz cloaking. *New J. Phys.* **2013**, *15*, 123029.
(22) Vakil, A.; Engheta, N. Transformation Optics Using Graphene. *Science* **2011**, *332*, 1291−1294.
(23) Vakil, A.; Engheta, N. Fourier optics on graphene. *Phys. Rev. B: Condens. Matter Mater. Phys.* **2012**, *85*, 075434.
(24) Gerhard, L.; Moyen, E.; Balashov, T.; Ozerov, I.; Portail, M.; Sahaf, H.; Masson, L.; Wulfhekel, W.; Hanbücken, M. A graphene electron lens. *Appl. Phys. Lett.* **2012**, *100*, 153106.
(25) Lu, J. Q.; Maradudin, A. A. Channel plasmons. *Phys. Rev. B: Condens. Matter Mater. Phys.* **1990**, *42*, 11159−11165.
(26) Gramotnev, D. K.; Pile, D. F. P. Single-mode subwavelength waveguide with channel plasmon-polaritons in triangular grooves on a metal surface. *Appl. Phys. Lett.* **2004**, *85*, 6323.
(27) Bozhevolnyi, S. I.; Volkov, V. S.; Devaux, E.; Ebbesen, T. W. Channel Plasmon-Polariton Guiding by Subwavelength Metal Grooves. *Phys. Rev. Lett.* **2005**, *95*, 046802.
(28) Volkov, V. S.; Bozhevolnyi, S. I.; Devaux, E.; Laluet, J.-Y.; Ebbesen, T. W. Wavelength Selective Nanophotonic Components Utilizing Channel Plasmon Polaritons. *Nano Lett.* **2007**, *7*, 880−884.
(29) Moreno, E.; Rodrigo, S. G.; Bozhevolnyi, S. I.; Martín-Moreno, L.; García-Vidal, F. J. Guiding and Focusing of Electromagnetic Fields with Wedge Plasmon Polaritons. *Phys. Rev. Lett.* **2008**, *100*, 023901.
(30) Bozhevolnyi, S. I.; Nerkararyan, K. V. Analytic description of channel plasmon polaritons. *Opt. Lett.* **2009**, *34*, 2039.
(31) Dintinger, J.; Martin, O. J. Channel and wedge plasmon modes of metallic V-grooves with finite metal thickness. *Opt. Express* **2009**, *17*, 2364.
(32) Gramotnev, D. K.; Bozhevolnyi, S. I. Plasmonics beyond the diffraction limit. *Nat. Photonics* **2010**, *4*, 83−91.
(33) Lee, S.; Kim, S. Long-range channel plasmon polaritons in thin metal film V-grooves. *Opt. Express* **2011**, *19*, 9836.
(34) Farhat, M.; Guenneau, S.; Bağcı, H. Exciting Graphene Surface Plasmon Polaritons through Light and Sound Interplay. *Phys. Rev. Lett.* **2013**, *111*, 23740.
(35) Schiefele, J.; Pedrós, J.; Sols, F.; Calle, F.; Guinea, F. Coupling Light into Graphene Plasmons through Surface Acoustic Waves. *Phys. Rev. Lett.* **2013**, *111*, 237405.
(36) Savin, A. V.; Kivshar, Y. S. Localized modes in capped single-walled carbon nanotubes. *Appl. Phys. Lett.* **2009**, *94*, 111903.
(37) Valle, G. D.; Longhi, S. Geometric potential for plasmon polaritons on curved surfaces. *J. Phys. B: At., Mol. Opt. Phys.* **2010**, *43*, 051002.
(38) Batz, S.; Peschel, U. Linear and nonlinear optics in curved space. *Phys. Rev. A: At., Mol., Opt. Phys.* **2008**, *78*, 043821.
(39) Schultheiss, V. H.; Batz, S.; Szameit, A.; Dreisow, F.; Nolte, S.; Tünnermann, A.; Longhi, S.; Peschel, U. Optics in Curved Space. *Phys. Rev. Lett.* **2010**, *105*, 143901.
(40) Batz, S.; Peschel, U. Solitons in curved space of constant curvature. *Phys. Rev. A: At., Mol., Opt. Phys.* **2010**, *81*, 053806.
(41) Kravets, V. G.; Grigorenko, A. N.; Nair, R. R.; Blake, P.; Anissimova, S.; Novoselov, K. S.; Geim, A. K. Spectroscopic ellipsometry of graphene and an exciton-shifted van Hove peak in absorption. *Phys. Rev. B: Condens. Matter Mater. Phys.* **2010**, *81*, 155413.
(42) Gorbach, A. V. Nonlinear graphene plasmonics: Amplitude equation for surface plasmons. *Phys. Rev. A: At., Mol., Opt. Phys.* **2013**, *87*, 013830.
(43) Auditore, A.; De Angelis, C.; Locatelli, A.; Boscolo, S.; Midrio, M.; Romagnoli, M.; Capobianco, A.-D.; Nalesso, G. Graphene sustained nonlinear modes in dielectric waveguides. *Opt. Lett.* **2013**, *38*, 631.
(44) Smirnova, D. A.; Gorbach, A. V.; Iorsh, I. V.; Shadrivov, I. V.; Kivshar, Y. S. Nonlinear switching with a graphene coupler. *Phys. Rev. B: Condens. Matter Mater. Phys.* **2013**, *88*, 045443.
(45) Smirnova, D. A.; Shadrivov, I. V.; Smirnov, A. I.; Kivshar, Y. S. Dissipative plasmon-solitons in multilayer graphene. *Laser Photon. Rev.* **2014**, *8*, 291−296.
(46) Kivshar, Y. S.; Agrawal, G. A. *Optical Solitons: From Fibers to Photonic Crystals*; Academic: San Diego, 2003.
(47) Gao, Y.; Ren, G.; Zhu, B.; Liu, H.; Lian, Y.; Jian, S. Analytical model for plasmon modes in graphene-coated nanowire. *Opt. Express* **2014**, *22*, 24322.
(48) Levy, N.; Burke, S. A.; Meaker, K. L.; Panlasigui, M.; Zettl, A.; Guinea, F.; Neto, A. H. C.; Crommie, M. F. Strain-Induced Pseudo-Magnetic Fields Greater Than 300 T in Graphene Nanobubbles. *Science* **2010**, *329*, 544−547.

DOI: 10.1021/acsphotonics.6b00116
ACS Photonics 2016, 3, 875−880